Barhl2 limits growth of the diencephalic primordium through Caspase3 inhibition of beta-catenin activation

Hugo Juraver-Geslin, Jérome Ausseil, Marion Wassef, Beatrice Claude Durand

Barhl2 limits growth of the diencephalic primordium through Caspase3 inhibition of β-catenin activation

Hugo A. Juraver-Geslin[a], Jérome J. Ausseil[b], Marion Wassef[a], and Béatrice C. Durand[a,1]

[a]Institut de Biologie de l'Ecole Normale Supérieure, Centre National de la Recherche Scientifique, Unité Mixte de Recherche 8197, Institut National de la Santé et de la Recherche Médicale U1024, 75005 Paris, France; and [b]Laboratoire de Biochimie, Centre Hospitalier Universitaire Nord et Faculté de Médecine et de Pharmacie, Institut National de la Santé et de la Recherche Médicale ERI12, Université de Picardie Jules Verne, 80000 Amiens, France

Edited by Igor B. Dawid, National Institute of Child Health and Human Services, Bethesda, MD, and approved December 30, 2010 (received for review September 21, 2010)

Little is known about the respective contributions of cell proliferation and cell death to the control of vertebrate forebrain growth. The homeodomain protein *barhl2* is expressed in the diencephalons of *Xenopus*, zebrafish, and mouse embryos, and we previously showed that Barhl2 overexpression in *Xenopus* neuroepithelial cells induces Caspase3-dependent apoptosis. Here, *barhl2* is shown to act as a brake on diencephalic proliferation through an unconventional function of Caspase3. Depletion of Barhl2 or Caspase3 causes an increase in diencephalic cell number, a disruption of the neuroepithelium architecture, and an increase in Wnt activity. Surprisingly, these changes are not caused by decreased apoptosis but instead, are because of an increase in the amount and activation of β-catenin, which stimulates excessive neuroepithelial cell proliferation and induces defects in β-catenin intracellular localization and an up-regulation of *axin2* and *cyclinD1*, two downstream targets of β-catenin/T-cell factor/lymphoïd enhancer factor signaling. Using two different sets of complementation experiments, we showed that, in the developing diencephalon, Caspase3 acts downstream of Barhl2 in limiting neuroepithelial cell proliferation by inhibiting β-catenin activation. Our data argue that Bar homeodomain proteins share a conserved function as cell type-specific regulators of Caspase3 activities.

cell-cycle | zona limitans intrathalamica | neuroarchitecture | apical

The forebrain (telencephalon and diencephalon) is derived from the most anterior part of the neural plate. Whereas the telencephalon grows rapidly during development, the diencephalon grows less, and its allosteric growth pattern plays a part in the formation of the zona limitans intrathalamica (ZLI), an important secondary brain organizer that secretes Sonic hedgehog (Shh; reviewed in refs. 1 and 2). Although much is known about the molecular processes underlying the acquisition of regional identity in the developing forebrain, little is known about how the differential growth of these subdomains is controlled.

In general, the growth of a developing tissue depends on cell growth and proliferation counterbalanced by programmed cell death, usually apoptosis (reviewed in ref. 3). Targeted disruption of one intracellular effector of the apoptotic pathway Caspase3 (Casp3) causes a decrease in apoptosis in the developing central nervous system (CNS), which is associated with hyperplasia of the ventricular and/or mantle zone and disorganization of the brain (4; reviewed in refs. 5 and 6). Caspases, however, function in processes other than apoptosis (reviewed in ref. 7). A non-apoptotic role for Casp3 in the regulation of cell proliferation and differentiation is suggested by its ability to cleave substrates associated with cell-cycle control and to finely tune mitogenic pathways (reviewed in ref. 7; 8, 9). Such observations raise the possibility that Casp3 may have nonapoptotic functions in neuroepithelial cells, where it might help control the proliferation and differentiation of CNS progenitor cells. Barhl1 and Barhl2 are homeodomain proteins that are highly conserved among metazoan species. In vertebrates, the *barhl* genes function in the acquisition of neural identity in the retina, specification of commissural neurons, cell migration in the cerebellum and hindbrain, and cell survival in the developing cochlea, cerebellum, and neuroepithelium (10–16; reviewed in ref. 17). We previously showed that *barhl2* is normally expressed in the *Xenopus* neural plate and the diencephalon. We also showed that specific depletion of Barhl2 or overexpression of human *bcl2* indirectly affects neural plate size by increasing the survival of midline cells that express Chordin, a bone morphogenetic protein (BMP) inhibitor, and Shh (18).

In the present study, we investigate the roles of Barhl*2* and Casp3 in relation to apoptosis and the differential growth of the forebrain primordium along its antero-posterior axis in the *Xenopus* embryo. We show that the depletion of either Barhl2 or Casp3 in embryos results in hyperplasia and cellular disorganization of the diencephalic neuroepithelium. Analysis of apoptotic cell distribution and the phenotype of Bcl-X_L–overexpressing embryos shows that Casp3 requirement for normal growth and patterning of these brain regions involves its influence on cell proliferation rather than apoptosis. We show that the amounts of total β-catenin and its active form are dramatically increased in the brains of both Barhl2- and Casp3-depleted embryos. In these embryos, the apical localization of β-catenin and the neuroepithelial architecture are disrupted. The increase in β-catenin is associated with the up-regulation of downstream targets of β-catenin/T-cell factor (TCF)/lymphoïd enhancer factor (LEF) signaling, *axin2*, and the cell-cycle regulator, *cyclin-D1* (*ccnd1*). Depletion of β-catenin through morpholino (MO) injection or overexpression of glycogen synthase kinase-3β (*gsk3β*) (19) that inhibits β-catenin activation rescues the proliferative defect observed in Barhl2- and Casp3-depleted embryos. In these embryos, the architectural defect is partially rescued through β-catenin depletion. We further show that Casp3 is epistatic to Barhl2 during β-catenin activation using two sets of complementation experiments.

Results

Influence of Barhl2 or Casp3 Depletion on Neuroepithelial Hyperplasia and Cell Death. At stage (st) 26/27, we detected *barhl2* expression in a ring of neuroectodermal cells in prosomere P2 (Fig. 1*Aa*). Both the thalamus and the pineal gland (red star in Fig. 1*A b–d*), which we used as a morphological landmark, develop from prosomere P2. *wnt3A* colocalized with *barhl2* in the alar plate of prosomere P2 (compare Fig. 1*A a–c*). This coexpression domain corresponds to the site where the ZLI will develop, and its boundary coincided precisely with the rostral border of *barhl2* and *wnt3a* expression (Fig. 1*A b* and *c*). At later stages, the *barhl2* area of expression spreads into the telencephalon and the mid-

Author contributions: M.W. and B.C.D. designed research; H.A.J.-G., J.J.A., and B.C.D. performed research; H.A.J.-G. and B.C.D. analyzed data; and M.W. and B.C.D. wrote the paper.

The authors declare no conflict of interest.

This article is a PNAS Direct Submission.

[1]To whom correspondence should be addressed. E-mail: bedurand@biologie.ens.fr.

This article contains supporting information online at www.pnas.org/lookup/suppl/doi:10.1073/pnas.1014017108/-/DCSupplemental.

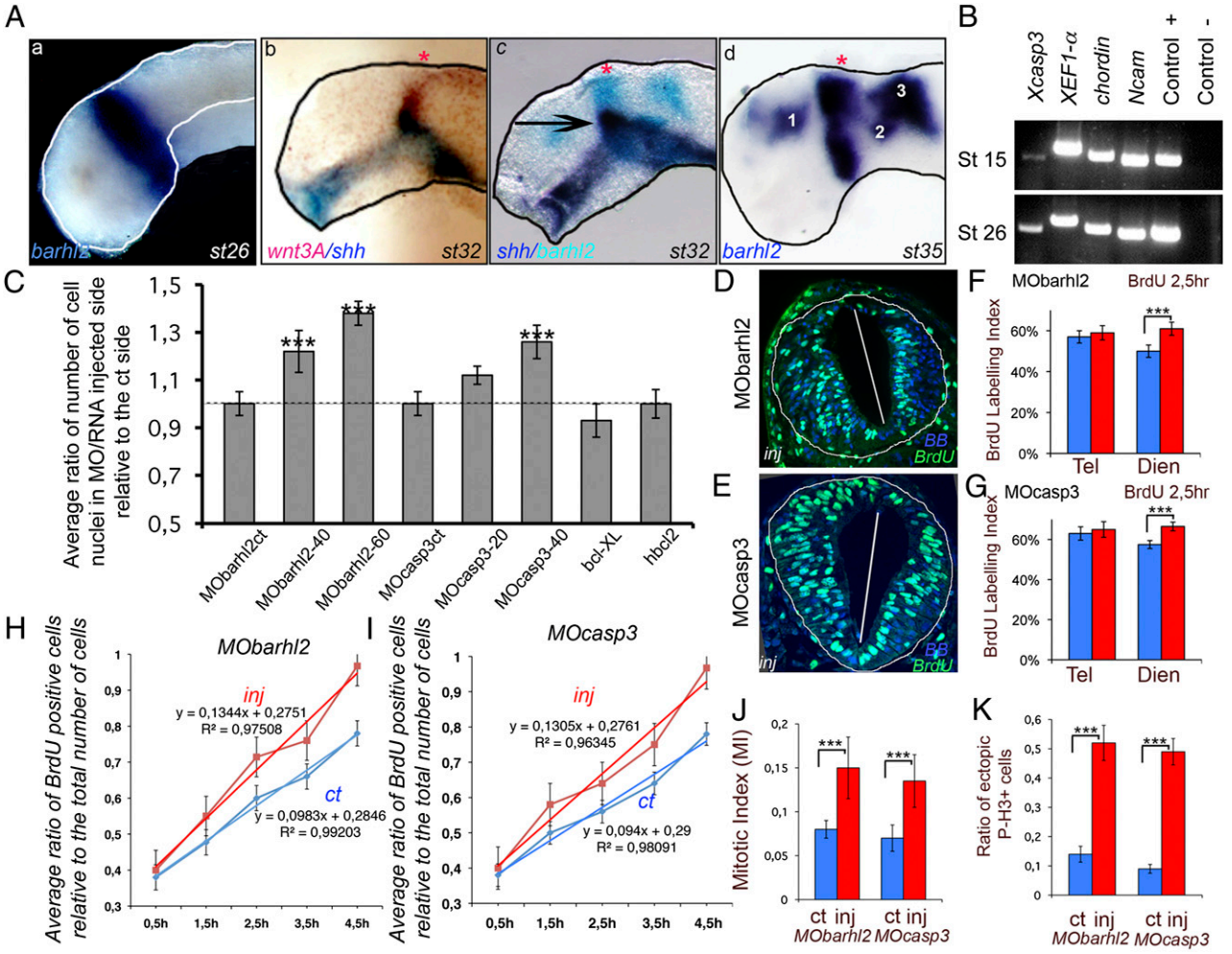

Fig. 1. Barhl2 or Casp3 depletion influence on neural tube hyperplasia, cell-cycle length, and neuroepithelium architecture. (*A*) barhl2 is expressed in the prosomere P2. ISH or double ISH on dissected neural tubes. (*a*) At st 26, barhl2 is expressed at the epichordal–prechordal border in the alar and basal plates of the neural tube. (*b*) At st 31 and 32, barhl2 expression overlaps with that of wnt3A (compare *b* and *c*). (*c*) The barhl2 rostral border of expression coincides with the rostral border of the ZLI (black arrow). (*d*) At st 33, barhl2 is expressed in the prospective diencephalon in the prospective pallium (1), the medial part of the pretectum (2), and the dorsal mesencephalon and future cerebellum (3). The pineal gland is indicated with a red star. (*B*) casp3 is expressed in the neural plate (st 15) and neural tube (st 26). RT-PCR analysis. chordin and Ncam are mesodermal and neuroectodermal markers, respectively. XEF-1α and the plasmid encoding Casp3 were used as positive controls, and water was the negative ct. (*C*) Average ratio of the number of nuclei on the MO/RNA-injected side of the neural tube relative to that on the ct side. Embryos were injected with MObarhl2, MOcasp3, bcl-X_L, or hbcl2 cRNA. The dotted line indicates a ratio of 1. MObarhl2ct (n = 3); MObarhl2-40 (40 ng; n = 6); MObarhl3-60 (60 ng; n = 7); MOcasp3ct (n = 3); MOcasp3-20 (20 ng; n = 5); MOcasp3-40 (40 ng; n = 8); bcl-X_L (n = 5); hbcl2 (n = 4). The differences in Rinj/ct between MObarhl2ct and MObarhl2-60 ($P \leq 0.033$), MObarhl2ct and MObarhl2-40 ($P \leq 0.06$), and MOcasp3ct and MOcasp-40 ($P \leq 0.036$) are significant. (*D*–*G*) BrdU labeling index (LI). (*D* and *E*) Representative st 26 diencephalic sections immunostained for BrdU (green) merged with bisbenzimide (BB; blue). BrdU LI was measured in st 26 forebrain neuroepithelium in (*F*) Barhl2- and (G) Casp3-depleted sections. (*F*) MObarhl2-injected embryos: telencephalon (ct vs. inj; n = 5, $P \leq 0.41$) and diencephalon (ct vs. inj; n = 9, $P \leq 0.0001$). (*G*) MOcasp3-injected embryos: telencephalon (ct vs. inj; n = 5, $P \leq 0.141$) and diencephalon (ct vs. inj; n = 9, $P \leq 0.0001$). ct, ct side; inj, injected side. (*H* and *I*) BrdU cumulative analysis. In st 26 diencephalic neuroepithelium, the cumulative BrdU incorporation rate measured as the slope of the linear regression function is higher in the injected side (red) vs. the ct side (blue) of (*H*) MObarhl2-injected (0.130 vs. 0.094; $n \geq 4$ for each time point) or (*I*) MOcasp3-injected (0.1344 vs. 0.098; $n \geq 4$ for each time point) embryos. H, hours. The average cell-cycle length, as described by *Tc* value, decreases in both MObarhl2- (*Tc* = 6.9 ± 0.64 h) and MOcasp3-injected (*Tc* = 7.1 ± 0.64 h) cells compared with noninjected cells (*Tc* = 8.7 ± 0.65 h and *Tc* = 8.9 ± 0.65 h), respectively. The changes in *Tc* observed among different types of cells are not affected by *Ts*, the duration of the S phase, which is always evaluated at 1.54 ± 0.28 h. (*J*) Mitotic index. MObarhl2 (ct vs. inj; n = 8, $P \leq 0.008$) and MOcasp3 (ct vs. inj; n = 8, $P \leq 0.001$). (*K*) Ratio of ectopic mitotic figures. Ratio of $P\text{-}^3H$–positive cells outside the ependymal zone (at least two cellular diameters) relative to the total number of mitotic cells. MObarhl2 (n = 8, $P \leq 0.0001$) and MOcasp3 (n = 7, $P \leq 0.0001$).

brain (Fig. 1*Ad*). We checked for the presence of *casp3* mRNA at similar stages using both in situ hybridization (ISH) (Fig. S1) and RT-PCR on extracts of dissected neuroectoderm of st 13–15 embryos and on the anterior fragments of dissected neural tubes of st 26 embryos (Fig. 1*B* and Fig. S1). *Casp3* mRNA was detected at both stages and coexpressed with *barhl2* in the prosomere P2 (Fig. S1). TUNEL staining was used to monitor the pattern of apoptosis during early *Xenopus* CNS development. Apoptotic nuclei were observed to be uniformly distributed and not confined to any specific area in the anterior neural tube from st 20 to 33 (Fig. S2). In agreement with previous observations, overexpression of *bcl-X_L* (Fig. S2) or *hbcl2* (20) cRNA protects anterior neural tube cells from apoptosis, at least up to st 26.

To determine the functions of Barhl2 and Casp3 in the diencephalon, we inhibited the activity of these proteins using antisense MO and followed the development of the diencephalic neuroepithelium at st 26/27. Barhl2 activity was inhibited using a previously characterized MO (*MObarhl2*) (18), and we designed

and validated two MOs for Casp3 (Fig. S3). We injected *MObarhl2* and *MOcasp3*, together with cRNA encoding for a tracer, into one dorsal blastomere of four-cell stage embryos. Both Barhl2- and Casp3-depleted embryos exhibited a dose-dependent enlargement of the neuroepithelium on the MO-injected side (Fig. S4). We quantified the enlargement of the diencephalon by calculating the ratio of the number of nuclei on the injected side (β-gal positive) to the number of nuclei on the control (ct) side (referred to as Rinj/ct). This ratio is significantly increased in Barhl2- and Casp3-depleted embryos (Fig. 1*C*). We did not observe any enlargement with the controls *MObarhl2ct* or *MOcasp3ct* (Fig. 1*C*). An unexpected effect of MO injection is cell death induced by p53 activation (21). Therefore, to assess whether apoptosis played a part in diencephalic growth before st 26, we injected *bcl-X_L* or *hbcl2* cRNA and monitored the effect on neural tube growth. We did not observe any change in the size of the neuroepithelium at st 26 in embryos in either case (Fig. 1*C* and Fig. S4).

Thus, from st 10.5 to 26, *barhl2* and *casp3* transcripts are detected in prosomere P2. Depletion of Barhl2 or Casp3 causes an overgrowth of the diencephalic neuroepithelium that does not result from a decrease in apoptosis.

Depletion of Barhl2 or Casp3 Increases Cell Proliferation in the Developing Diencephalon. We assessed whether depletion of Barhl2 or Casp3 modifies the pace of diencephalic neuroepithelial proliferation. We showed that, before st 26/27, all forebrain cells incorporated BrdU (Fig. S4). We exposed embryos to BrdU and determined (*i*) the BrdU labeling index (LI) and (*ii*) the proportion of phosphorylated histone H3 (P-H3)-positive cells, the mitotic index (MI), on the injected and ct sides of st 26 forebrain neuroepithelium. We observed that the depletion of either Barhl2 or Casp3 caused a significant increase in the diencephalic BrdU LI (Fig. 1 *D*–*G*) and the MI (Fig. 1*J*). No effects on the BrdU LI in the developing telencephalon were detected. By BrdU cumulative analysis, we showed that, at st 26, neuroepithelial cells depleted of Barhl2 (Fig. 1*H*) or Casp3 (Fig. 1*I*) undergo shorter cell cycles compared with ct progenitors. The slope of BrdU incorporation over time is higher in both *MObarhl2*- (Fig. 1*H*) and *MOcasp3*-injected sides (Fig. 1*I*) compared with their respective ct sides. In the proliferating neuroepithelium of normal vertebrate embryos, the nuclei of dividing cells migrate to the basal surface to undergo S phase and to the apical (ventricular) surface to undergo mitosis. In Barhl2- or Casp3-depleted st 26/27 embryos, both BrdU-positive nuclei and P-H3–positive cells were scattered throughout the neuroepithelial wall on the injected side (Fig. 1 *D* and *E* and Fig. S4). We quantified this effect by assessing the ratio of ectopic mitoses to the total number of mitoses and found that the injected side had five times more mitotic cells that were not bordering the ventricular lumen than did the ct side (Fig. 1*K* and Fig. S4).

Therefore, before st 26, both Barhl2 and Casp3 reduce diencephalic growth by limiting the rate of progenitor proliferation. Moreover, depletion of Barhl2 or Casp3 disorganizes the neuroepithelial architecture.

Depletion of Barhl2 or Casp3 Increases β-Catenin and Wnt Activity. We noticed that the defects in cell proliferation and the neuroepithelial structure in Barhl2- and Casp3-depleted *Xenopus* embryos seem similar to those described in mice with altered β-catenin levels and activity (reviewed in refs. 22 and 23). We, therefore, tested whether β-catenin and/or Wnt pathway activity could be affected by depletion of Barhl2 or Casp3.

We used Western blotting to analyze β-catenin levels and activity in extracts from the heads of st 26 embryos depleted for Barhl2 or Casp3. In both cases, there was an increase in total β-catenin and more dramatically, in its activated form (Fig. 2*A*). We confirmed that the active form of β-catenin is specifically enriched in nuclear st 26 head extracts (Fig. 2*B*). Immunohistochemistry (IHC) analysis revealed a severe disorganization of the β-catenin staining at the apical surface of *MObarhl2*- or *MOcasp3*-injected neuroepithelia compared with the ct side, which is associated with disruption of the neuroepithelium (Fig. 2*C* and Fig. S5). We followed the activity of the Wnt pathway with ISH for *axin2* and *ccnd1*, two downstream targets of the β-catenin/TCF/LEF signaling pathway (24, 25). We observed in Barhl2- (Fig. 2*D* and Fig. S5) or Casp3-depleted (Fig. 2*E* and Fig. S5) neuroepithelium an entent of *axin2* and *ccnd1* expression domains inside the prosomere P2 alar plate (compare Fig. 2 *D a* and *b* and *E a* and *b*; Fig. 2 *Dc* and *Ec* and Fig. S5).

We conclude that Casp3 and Barhl2 normally limit the accumulation and activation of β-catenin in *Xenopus* st 26 heads.

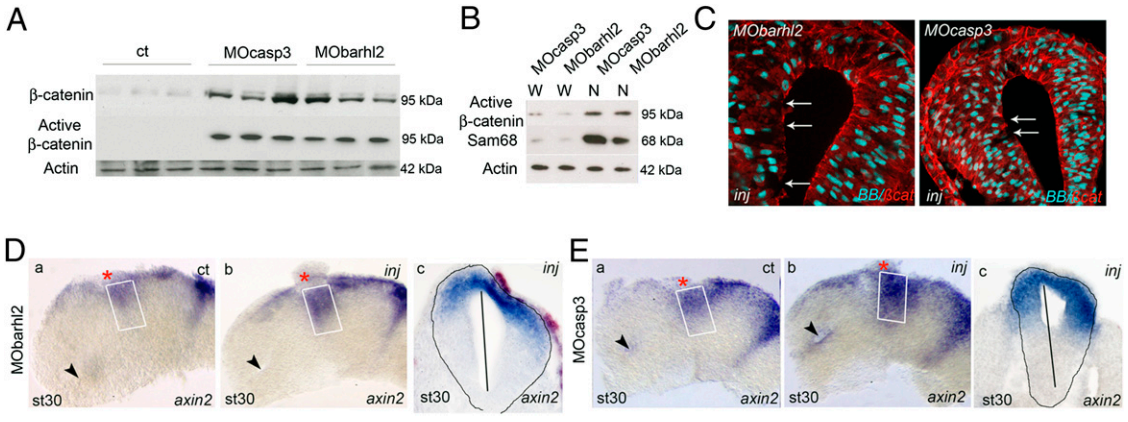

Fig. 2. Barhl2 and Casp3 depletion increases β-catenin and Wnt activity. (*A* and *B*) Western blot analysis. Proteins (10 μg) extracted from st 26 heads of embryos injected with GFP (ct), *MOcasp3*, or *MObarhl2*. α-actin (42 kDa) is used as a loading ct. (*A*) Barhl2- and Casp3-depleted head extracts exhibit a significant increase in both β-catenin and active β-catenin levels (95 kDa) as indicated. (*B*) Active β-catenin detected in *MOcasp3*- or *MObarhl2*-injected head extracts is enriched in nuclear head extracts (N) compared with that in whole-cell head extracts (W). Sam68 is used as a marker of proper nuclear proteins extraction. (*C*) β-catenin mislocalization. Representative IHC images for β-catenin (red) merged with BB (blue) on diencephalic sections of st 26/27 embryos injected with *MObarhl2* or *MOcasp3*. Arrows indicate the part of apical surfaces where β-catenin staining is disrupted. Inj, injected side. (*D* and *E*) Analysis of Wnt activity. *axin2* expression profiles at st 30 analyzed by ISH. The ct (*a*) and injected (*b*) sides of one representative dissected neural tube flat-mounted or (*c*) a section at the diencephalic level are shown. The percent of embryos exhibiting the phenotype is indicated. (*Da*) ct and (*Db* and *Dc*) Barhl2-depleted (80%, *n* = 15) and (*Ea*) ct and (*Eb* and *Ec*) Casp3-depleted neural tubes (78%, *n* = 18). The white rectangle delineates the prosomere P2 alar plate. The black arrow indicates localization of the optic stalk.

Depletion of either protein increases activity of the Wnt pathway in the dorsal prosomere P2 and affects β-catenin intracellular localization.

Effects of Barhl2 and Casp3 Depletion Are Rescued by Depletion of β-Catenin. We next investigated whether changes in β-catenin levels were responsible for the changes in the developing diencephalon in Barhl2- and Casp3-depleted embryos. We injected *MObarhl2* or *MOcasp3*, together with the previously characterized *MOβcat* (26), or cRNA encoding for *gsk3β* that phosphorylates and subsequently inhibits β-catenin activation. *MOβcat* and *gsk3β* cRNA were targeted to the anterior dorsal neural tube to minimize the depletion of β-catenin in the Spemann organizer.

As previously described, we evaluated (*i*) the enlargement of the diencephalic neuroepithelium by assessing the Rinj/ct and (*ii*) the disorganization of the neuroepithelium by counting the number of ectopic mitotic cells in the diencephalon. As expected and in contrast to *MObarhl2* and *MOcasp3* injections, when *MOβcat* or *gsk3β* cRNA were injected alone, we observed a decrease in the Rinj/ct (Fig. 3*D*). As an additional control, we injected a dominant negative form of *gsk3β, gsk3βDN* cRNA (19) and showed that it generated an increase in cell number in the diencephalon (Fig. 3*D*). When *MOβcat* alone was injected, 52% of mitotic cells were ectopically located (Fig. 3 *C* and *E*), and *gsk3β* overexpression induced a slight increase in mitotic cells located ectopically (Fig. 3*E*). *Axin2* expression was reduced in the P2 alar plate of both β-catenin–depleted (Fig. 3*F*) and Gsk3β-overexpressing (Fig. 3*G*) diencephalic neuroepithelium, confirming the Wnt pathway inhibitory activities of *MOβcat* and *gsk3β* cRNA. Coinjection of both *MObarhl2* and *MOcasp3* with either *MOβcat* or *gsk3β* cRNA showed a normalization of the diencephalic cell number on the injected side vs. the ct side (Fig. 3 *A*, *B*, and *D*). We also observed a significant decrease in the number of mitotic cells ectopically located in the diencephalon of *MObarhl2*/*MOβcat*- or *MOcasp3*/*MOβcat*-injected embryos compared with their respective ct sides (Fig. 3 *A*, *B*, and *E*). The rescue was cell autonomous and is shown by the correlation between the presence of the MO (GFP-positive cells) and the loss of apical membrane attachment of P-^{3}H–positive cells (Fig. 3 *A*–*C*). In contrast, under our experimental conditions, the neuroepithelium disorganization phenotype was not rescued by *gsk3β* overexpression (Fig. 3*E*). Finally, MO depletion of β-catenin reduced the expansion of the *axin2* expression domain in the P2 alar plate of Barhl2- (Fig. 3*H*) and Casp3-depleted (Fig. 3*I*) embryos (compare Fig. 3 *H a* and *b* and *I a* and *b*).

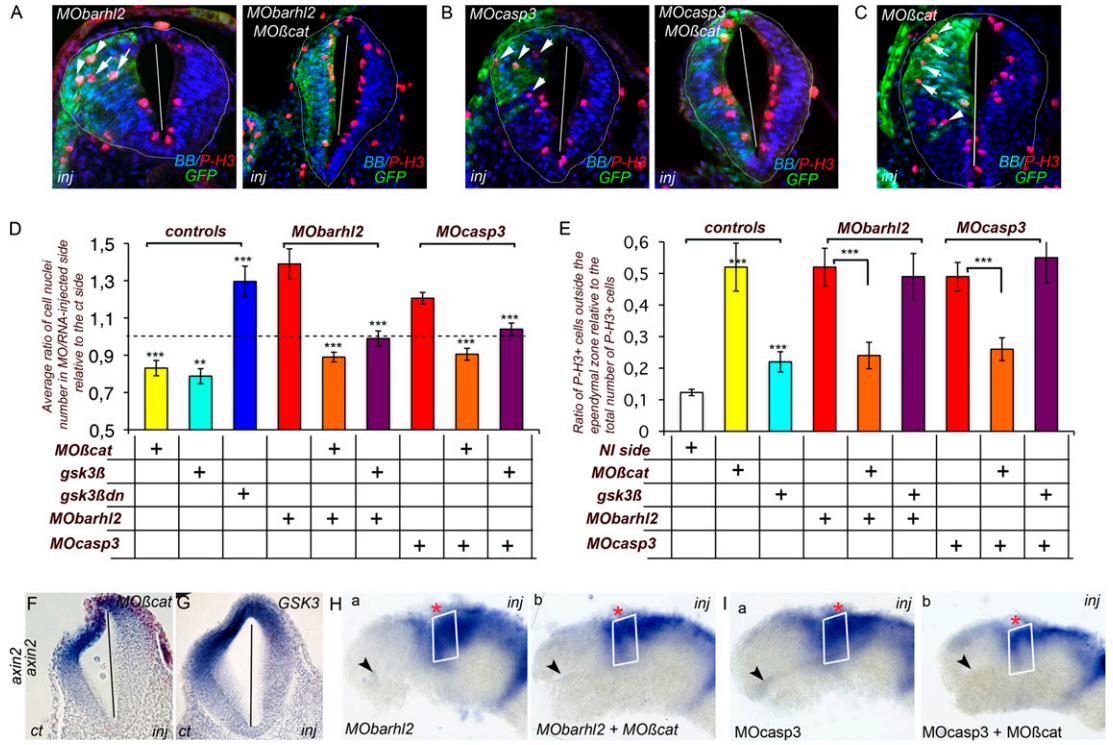

Fig. 3. Barhl2- and Casp3-depleted defects are rescued by inhibition of β-catenin activity. (*A*–*C*) Representative IHC. P-^{3}H (red) merged with BB (blue) and GFP (green) images on diencephalic sections of st 26/27 embryos injected with (*A*) *MObarhl2* or *MObarhl2/MOßcat*, (*B*) *MOcasp3* or *MOcasp3/MOßcat*, or (*C*) *MOßcat*. Inj, injected side. The white arrows indicate GFP^{+}/P-^{3}H^{+} cells detached from the apical membrane. (*D*) Normalization of Rinj/ct. The dotted line indicates a Rinj/ct of 1. *MOßcat* (n = 10); *gsk3β* (n = 8); *gsk3β-dn* (n = 4). *MObarhl2* (n = 5), *MObarhl2/MOßcat* (n = 13), *MObarhl2/gsk3β* (n = 8); *MOcasp3* (n = 8), *MOcasp3/MOßcat* (n = 8); *MOcasp3/gsk3β* (n = 4); ct vs. *MOßcat* ($P \leq 0.001$); ct vs. *gsk3β* ($P \leq 0.025$); ct vs. *gsk3β-dn* ($P \leq 0.005$); *MObarhl2* vs. *MObarhl2/MOßcat* ($P \leq 0.001$); *MObarhl2* vs. *MObarhl2/gsk3β* ($P \leq 0.011$); *MOcasp3* vs. *MOcasp3/MOßcat-10* ($P \leq 0.000$); *MOcasp3* vs. *MOcasp3/gsk3β* ($P \leq 0.002$). (*E*) Normalization of the ratio of ectopic mitosis. NI, noninjected. *MOßcat* (n = 5); *gsk3β* (n = 6); *MObarhl2* (n = 8), *MObarhl2/MOßcat* (n = 10), *MObarhl2/gsk3β* (n = 4), *MOcasp3* (n = 7) *MOcasp3/MOßcat* (n = 7), *MOcasp3/gsk3β* (n = 5); ct vs. *MOßcat* ($P \leq 0.005$); ct vs. *gsk3β* ($P \leq 0.007$); *MObarhl2* vs. *MObarhl2/MOßcat* ($P \leq 0.003$); *MObarhl2* vs. *MObarhl2/gsk3β* ($P \leq 0.665$); *MOcasp3* vs. *MOcasp3/MOßcat* ($P \leq 0.007$); *MOcasp3* vs. *MOcasp3/gsk3β* ($P \leq 0.604$); *MOßcat* vs. *MObarhl2/MOßcat* ($P \leq 0.01$); *MOßcat* vs. *MOcasp3/MOßcat* ($P \leq 0.015$). (*F*–*I*) Normalization of Wnt activity. *axin2* expression profile of st 30-injected neural tubes analyzed by ISH. (*F* and *G*) Representative embryos are shown either as the diencephalic section or (*H* and *I*) the ct (a) and injected (b) sides of one representative dissected neural tube mounted flat. At st 30 in the P2 alar plate, *axin2* expression territory is reduced in *MOßcat*-depleted (*F*; 73%, n = 15) and *gsk3β* overexpressing (*G*; 75%, n = 12) embryos. The P2 alar plate (white rectangle) *axin2* expression territory is reduced in both *MObarhl2/MOßcat*- (compare *H a* and *b*; 66%, n = 18) and *MOcasp3/MOßcat*-injected (compare *I a* and *b*; 65%, n = 38) sides compared with the *MObarhl2*- and *MOcasp3*-injected and respective ct sides. The black arrow indicates the optic stalk.

Hence, depletion of β-catenin through MO injection or reduction of β-catenin activation through overexpression of Gsk3β rescues the hyperproliferative defect observed in Barhl2- and Casp3-depleted embryos. The neuroepithelium structural defect is saved through *MOßcat* injection.

Casp3 Acts Downstream of Barhl2 in Limiting Wnt Pathway Activation. Considering that Barhl2- and Casp3-depleted embryos exhibit similar anterior neural tube developmental defects, we tested whether the two proteins acted in the same pathway or in parallel. We investigated whether we could complement the diencephalic increase in cell number observed in Barhl2-depleted embryos through *caspase3* overexpression and vice versa. We targeted *casp3* and *barhl2* cRNA to the anterior dorsal neural tube. When *MObarhl2* was coinjected with *casp3* cRNA, we observed a decrease in the Rinj/ct (Fig. 4*A*). Conversely, we did not measure any significant difference in the Rinj/ct between *MOcasp3*- and *MOcasp3*/*barhl2*-injected embryos (Fig. 4*A*). We followed the activity of the Wnt-reporter construct TOP-Flash that carries Tcf-binding sites upstream of the luciferase reporter gene (27) in animal cap (AC) explants anteriorized with the BMP inhibitor noggin cRNA. Using RT-PCR analysis, we confirmed that these explants behave similarly to st 20 anterior neuroectoderm (Fig. S6). Mean luciferase activities relative to Tcf binding sites-cfos-promoter-firefly-luciferase (TOP-Flash) were measured in ACs prepared from embryos injected with *MObarhl2* alone or together with *casp3* cRNA or with *MOcasp3* alone or together with *barhl2* cRNA. We observed a significant 2- or 1.8-fold increase of TOP-Flash activity on depletion of Barhl2 and Casp3, respectively (Fig. 4*B*). The coinjection of *casp3* RNA together with *MObarhl2* significantly diminished TOP-Flash activity from 2- to 1.4-fold (Fig. 4*B*). Coinjection of *barhl2* RNA together with *MOcasp3* does not affect TOP-Flash activity (Fig. 4*B*). We did not observe any of these activity changes using the Tcf mutated binding sites-cfos-promoter-firefly-luciferase (FOP-Flash) reporter that is an altered version of TOP-Flash carrying point mutations in the Tcf-binding sites (27).

We conclude that Barhl2 and Casp3 act upstream of the Tcf-binding factors such as β-catenin and that Casp3 acts downstream of Barhl2 in the molecular cascade that limits Wnt pathway activation in the *Xenopus* diencephalic primordium.

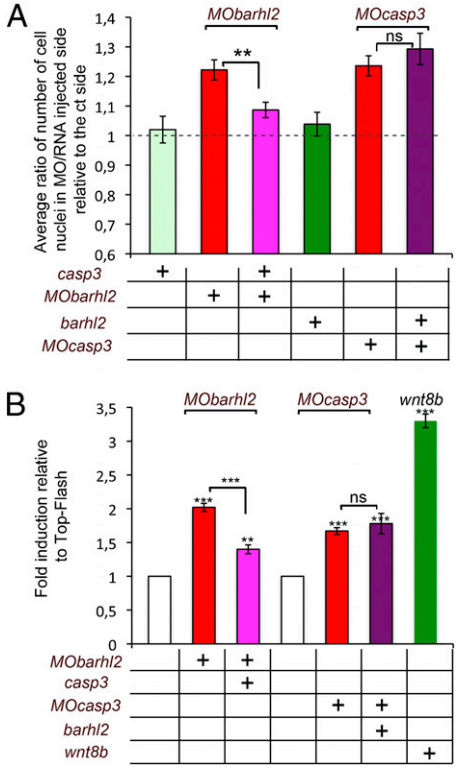

Fig. 4. Casp3 acts downstream of Barhl2 in limiting Wnt pathway activation. (*A*) Diencephalic enlargement complementation. Embryos were injected with MObarhl2-40, MOcasp3-40, casp3, or barhl2 cRNA as indicated. Rinj/ct is shown. The dotted line indicates a ratio of 1. *n*, number of sections analyzed. MObarhl2-40 ($n = 41$); MOcasp3-40 ($n = 28$); casp3 ($n = 31$); barhl2 ($n = 26$); MObarhl2-40 together with casp3 ($n = 41$); MOcasp3-40 together with barhl2 ($n = 41$). The differences in Rinj/ct between MObarhl2-40 and MObarhl2-40/casp3 are significant ($P \leq 0.016$); the difference between MOcasp3-40 and MOcasp3-40/barhl2 is not ($P \leq 0.416$). (*B*) TOP-Flash induction complementation. Fold induction relative to TOP-Flash is shown. *n*, number of AC analyzed. TOP-Flash ($n = 75$), MObarhl2-40 ($n = 48$); MObarhl2-40 with casp3 ($n = 54$); MOcasp3-40 ($n = 42$); MOcasp3-40 with barhl2 ($n = 42$); wnt8b ($n = 18$). The differences in relative activity between respective controls and MObarhl2-40 ($P \leq 0.001$), MObarhl2-40/casp3 ($P \leq 0.015$), MOcasp3-40 ($P \leq 0.006$), MOcasp3-40/barhl2 ($P \leq 0.037$), wnt8b ($P \leq 0.002$), and MObarhl2-40 and MObarhl2-40/casp3 ($P \leq 0.001$) are all significant in contrast to the difference in fold activity between MOcasp3-40 and MOcasp3-40/barhl2 ($P \leq 0.656$). Ns, not significant.

Discussion

In this study, we show that the homeodomain-containing protein Barhl2 and Casp3 normally limit the rate of proliferation of diencephalic progenitors, at least in part by directly or indirectly limiting the amount and/or the activation of β-catenin. We provide evidence that Casp3 acts downstream of Barhl2 in reducing activation of the canonical Wnt signaling pathway (Fig. S7). We establish that the role of Casp3 in *Xenopus* diencephalon growth does not depend on its apoptosis effector function.

Casp3 Inhibits the Proliferation of Diencephalic Neural Progenitor Cells by Decreasing β-Catenin Activity. We find that overexpression of Bcl-X_L or hBcl2, which can protect neuroepithelial cells from apoptosis at least up to st 28 in *Xenopus* embryos (our study and ref. 20), has no effect on forebrain growth. Therefore, Casp3 and Bcl-X_L have independent functions during *Xenopus* forebrain development. Inactivation of the mouse *casp3* gene causes overgrowth and disorganization of the brain, which first appears in the diencephalic walls (4), a phenotype similar to that in Casp3-depleted *Xenopus* embryos. This suggest that the role of Casp3 in regulating the proliferation of neuroepithelial cells during diencephalon development, independent of its role in apoptosis, is conserved in most vertebrates.

Our findings show that, during forebrain development, Casp3 directly or indirectly reduces activation of the canonical Wnt pathway. This regulation seems cell-autonomous and at least partly mediates the ability of Casp3 to limit diencephalic growth. Similarly, fly caspases have been reported to influence the fate of sensory organ precursor cells by antagonizing the wg pathway. Cleavage-dependent activation of a Gsk-3β isoform (shaggy) by the fly caspases Dronc or Drice leads to the downstream phosphorylation and subsequent inhibition of β-catenin activation and the wg pathway (8).

We find that depletion of either Casp3 or β-catenin alters the attachment of cells in mitosis to the apical surface. In agreement with our and published observations (reviewed in ref. 28), we suggest that increasing (*MOcasp3*) or decreasing (*MOßcat*) the intracellular amount of β-catenin interferes with correct formation of the adherens junctions localized at the apical end of neuroepithelial cells. Disruptions in such junctions alter the internal structure of the neuroepithelium (29). This hypothesis is consistent with our data showing that depletion of β-catenin partly rescues the architectural neuroepithelium defect in Casp3-depleted embryos and vice versa.

Barhl2: A Genetic Regulator of Diencephalic Growth. Our findings show that Barhl2 acts as a brake on diencephalic growth in *Xenopus*. The phenotypes of Barhl2- and Casp3-depleted embryos are remarkably similar in terms of defects in neuroepithelial growth, organization, and gene expression. We observe that Casp3 depletion protects st 14 neuroepithelial cells from Barhl2-induced apoptosis. Overexpression of Casp3 compensates for the Barhl2 depletion phenotypes, whereas Barhl2 overexpression is inactive with respect to the Casp3 depletion defects. Taken together, these data provide evidence that Casp3 acts downstream of Barhl2 in controlling diencephalic neuroepithelial growth. In agreement with these observations, the *Caenorhabditis elegans* Bar ortholog CEH-30 defines a checkpoint that integrates both sex determination and cell fate determination/survival signals to control the activation of the cell death program in a male-specific chemosensory neuron (CEM), probably by regulating the expression or activation of key cell death genes (30, 31).

Very little is known about the molecular basis underlying the ability of Casp3 to act in multiple ways (reviewed in ref. 7). In *C. elegans*, *barhl1* and *barhl2* transgenes rescue the CEM survival defect of male *ceh-30* mutants, showing that these genes encode proteins that retain the functions and target specificity of CEH-30 (30). It is, therefore, possible that Barhl2 controls Casp3 proteolytic activity and specificity by direct interaction; alternatively, Barhl2 could regulate the transcription of genes that encode regulators of Casp3 activity in neuronal development independently of cell death. We suggest that the *C. elegans* and vertebrate Bar homeodomain proteins share a conserved function as cell type-specific regulators of Casp3 activities.

Barhl2 and Casp3 Are Intracellular Regulators of the Canonical Wnt Pathway. At st 26 *wnt3a*, an activator of the Wnt canonical pathway is expressed in the diencephalic P2 alar plate. In this same domain, when Casp3 and Barhl2 are depleted, we observe an extent of the *axin2* or *ccnd1* expression territory. This enlargement is diminished by depletion of β-catenin. Taken together, our data argue for a Barhl2-controlled Wnt activity regulatory loop in the P2 alar plate territory. Numerous observations have suggested a specific function for the canonical Wnt pathway in diencephalon growth. Wnt3 and Wnt3A are expressed at the posterior border of the ZLI, where they form a regulatory loop with Shh to help control the growth and patterning of the P2 alar plate (32). We suggest that Barhl2 plays a part in establishment of the specific diencephalic growth pattern that is at play during formation of the ZLI (33).

Materials and Methods

See *SI Materials and Methods* for embryos and injection set ups, antisense MOs and RT-PCR primers sequences, and antibodies references as well as a description of all experimental protocols used during this study. For information regarding confocal microscopy, images, statistical analysis, and associated references, see *SI Materials and Methods*.

ACKNOWLEDGMENTS. We thank Anne-Hélène Monsoro-Burq, Muriel Perron, Muriel Umbhauer, David Dupasquier, and Thomas Pietri for their comments on the manuscript and Said Maallem for help with statistical analysis. B.C.D. expresses her gratitude to Martin Raff and Kathleen Smith for their editing work on the manuscript. This work was supported by the Centre National de la Recherche Scientifique (Centre National de la Recherche Scientifique/Ecole Normale Supérieure Unité Mixte de Recherche 8542), a grant from the Agence Nationale de la Recherche (ANR) (SWITCH project), and Association pour la Recherche sur le Cancer (ARC) Grants 4972 and 5115 (to M.W.).

1. Kiecker C, Lumsden A (2004) Hedgehog signaling from the ZLI regulates diencephalic regional identity. *Nat Neurosci* 7:1242–1249.
2. Echevarria D, Vieira C, Gimeno L, Martinez S (2003) Neuroepithelial secondary organizers and cell fate specification in the developing brain. *Brain Res Brain Res Rev* 43:179–191.
3. Conlon I, Raff M (1999) Size control in animal development. *Cell* 96:235–244.
4. Kuida K, et al. (1996) Decreased apoptosis in the brain and premature lethality in CPP32-deficient mice. *Nature* 384:368–372.
5. Kuan CY, Roth KA, Flavell RA, Rakic P (2000) Mechanisms of programmed cell death in the developing brain. *Trends Neurosci* 23:291–297.
6. Oppenheim RW, et al. (2001) Programmed cell death of developing mammalian neurons after genetic deletion of caspases. *J Neurosci* 21:4752–4760.
7. Yi CH, Yuan J (2009) The Jekyll and Hyde functions of caspases. *Dev Cell* 16:21–34.
8. Kanuka H, et al. (2005) Drosophila caspase transduces Shaggy/GSK-3beta kinase activity in neural precursor development. *EMBO J* 24:3793–3806.
9. Woo M, et al. (2003) Caspase-3 regulates cell cycle in B cells: A consequence of substrate specificity. *Nat Immunol* 4:1016–1022.
10. Ding Q, et al. (2009) BARHL2 differentially regulates the development of retinal amacrine and ganglion neurons. *J Neurosci* 29:3992–4003.
11. Chellappa R, et al. (2008) Barhl1 regulatory sequences required for cell-specific gene expression and autoregulation in the inner ear and central nervous system. *Mol Cell Biol* 28:1905–1914.
12. Saba R, Johnson JE, Saito T (2005) Commissural neuron identity is specified by a homeodomain protein, Mbh1, that is directly downstream of Math1. *Development* 132:2147–2155.
13. Poggi L, Vottari T, Barsacchi G, Wittbrodt J, Vignali R (2004) The homeobox gene Xbh1 cooperates with proneural genes to specify ganglion cell fate within the Xenopus neural retina. *Development* 131:2305–2315.
14. Mo Z, Li S, Yang X, Xiang M (2004) Role of the Barhl2 homeobox gene in the specification of glycinergic amacrine cells. *Development* 131:1607–1618.
15. Li S, Qiu F, Xu A, Price SM, Xiang M (2004) Barhl1 regulates migration and survival of cerebellar granule cells by controlling expression of the neurotrophin-3 gene. *J Neurosci* 24:3104–3114.
16. Colombo A, Reig G, Mione M, Concha ML (2006) Zebrafish BarH-like genes define discrete neural domains in the early embryo. *Gene Expr Patterns* 6:347–352.
17. Reig G, Cabrejos ME, Concha ML (2007) Functions of BarH transcription factors during embryonic development. *Dev Biol* 302:367–375.
18. Offner N, Duval N, Jamrich M, Durand B (2005) The pro-apoptotic activity of a vertebrate Bar-like homeobox gene plays a key role in patterning the Xenopus neural plate by limiting the number of chordin- and shh-expressing cells. *Development* 132:1807–1818.
19. Dominguez I, Itoh K, Sokol SY (1995) Role of glycogen synthase kinase 3 beta as a negative regulator of dorsoventral axis formation in Xenopus embryos. *Proc Natl Acad Sci USA* 92:8498–8502.
20. Yeo W, Gautier J (2003) A role for programmed cell death during early neurogenesis in xenopus. *Dev Biol* 260:31–45.
21. Robu ME, et al. (2007) p53 activation by knockdown technologies. *PLoS Genet* 3:e78.
22. Grigoryan T, Wend P, Klaus A, Birchmeier W (2008) Deciphering the function of canonical Wnt signals in development and disease: Conditional loss- and gain-of-function mutations of beta-catenin in mice. *Genes Dev* 22:2308–2341.
23. Chenn A, Walsh CA (2002) Regulation of cerebral cortical size by control of cell cycle exit in neural precursors. *Science* 297:365–369.
24. Jho EH, et al. (2002) Wnt/beta-catenin/Tcf signaling induces the transcription of Axin2, a negative regulator of the signaling pathway. *Mol Cell Biol* 22:1172–1183.
25. Shtutman M, et al. (1999) The cyclin D1 gene is a target of the beta-catenin/LEF-1 pathway. *Proc Natl Acad Sci USA* 96:5522–5527.
26. Heasman J, Kofron M, Wylie C (2000) Beta-catenin signaling activity dissected in the early Xenopus embryo: A novel antisense approach. *Dev Biol* 222:124–134.
27. Korinek V, et al. (1997) Constitutive transcriptional activation by a beta-catenin-Tcf complex in APC-/- colon carcinoma. *Science* 275:1784–1787.
28. Brembeck FH, Rosário M, Birchmeier W (2006) Balancing cell adhesion and Wnt signaling, the key role of beta-catenin. *Curr Opin Genet Dev* 16:51–59.
29. Kadowaki M, et al. (2007) N-cadherin mediates cortical organization in the mouse brain. *Dev Biol* 304:22–33.
30. Schwartz HT, Horvitz HR (2007) The C. elegans protein CEH-30 protects male-specific neurons from apoptosis independently of the Bcl-2 homolog CED-9. *Genes Dev* 21: 3181–3194.
31. Peden E, Kimberly E, Gengyo-Ando K, Mitani S, Xue D (2007) Control of sex-specific apoptosis in C. elegans by the BarH homeodomain protein CEH-30 and the transcriptional repressor UNC-37/Groucho. *Genes Dev* 21:3195–3207.
32. Ishibashi M, McMahon AP (2002) A sonic hedgehog-dependent signaling relay regulates growth of diencephalic and mesencephalic primordia in the early mouse embryo. *Development* 129:4807–4819.
33. Kiecker C, Lumsden A (2005) Compartments and their boundaries in vertebrate brain development. *Nat Rev Neurosci* 6:553–564.